Predictive Assessment of Surface Resistances in Zeolite Membranes Using Atomically Detailed Models

David A. Newsome and David S. Sholl*

Department of Chemical Engineering, Carnegie-Mellon University, Pittsburgh, Pennsylvania 15213

Received: December 17, 2004; In Final Form: February 11, 2005

The diffusive transport of molecules through nanoporous membranes is determined by both intracrystalline diffusion and mass transport resistances associated with entering and leaving the membrane material. We compare two methods for assessing the relative importance of these resistances based on atomically detailed descriptions of the membrane material. For extremely thin membranes, net transport can be assessed using dual control volume grand canonical molecular dynamics (DCV-GCMD). We show that previous implementations of this technique may have been influenced by nonisothermal effects in interfacial regions and suggest a simple remedy to this situation. We also introduce an approximate method that uses information only from equilibrium MD simulations, which avoids the significant computational expense associated with DCV-GCMD. This approximate method can be used to rapidly assess the importance of interface-related resistances to mass transport over broad ranges of membrane operating conditions. This method will be useful in allowing a rapid determination of whether these interface resistances are significant in practical experimental situations. These two methods are compared by considering the transport of CH_4 and CF_4 through defect-free silicalite membranes.

I. Introduction

Zeolites are a common class of inorganic crystalline materials that possess ordered atomic-scale porous networks. There is a considerable body of work on the uses of thin films of zeolites as membranes for separating gas or liquid mixtures.[1−4] One motivation underlying these efforts is the notion that the crystalline order imposed in the micropores of zeolites may offer greater control over flux and selectivity than can be achieved in materials such as polymers that have pore distributions that are inherently less well resolved. To exploit this observation effectively, it is necessary to have methods that directly link the structure of zeolite membranes with their performance under practical conditions.

Diffusion through zeolite membranes occurs in three steps. First, the guest molecule adsorbs from the feed phase to the membrane surface. Second, it diffuses through the zeolite that defines the membrane. Finally, the guest molecule must desorb from the pores and into the permeate phase. It is useful to define a separate mass transfer resistance for each of these three steps. The resistance to mass transfer in the zeolite is simply related to the intracrystalline diffusivity of the guest molecule. For thick enough membranes, this intracrystalline resistance dominates mass transfer. The interfacial mass transfer resistances due to the molecules entering and exiting the surface are referred to collectively as surface barriers.

One theme in recent work on zeolite membranes has been to predict the properties of idealized membranes using atomically detailed models of the membrane material and the interactions between adsorbed molecules and the membrane.[5−17] Work on this topic can be broadly divided into two approaches, those that directly simulate the entire extent of a membrane under nonequilibrium conditions[5−11,17−28] and the alternative method of using equilibrium molecular dynamics (EMD) simulations of adsorbates in a bulk zeolite to provide parametric input for a continuum description of a membrane.[12−14,16,29,30] We will refer to the first approach as direct methods.

The two classes of simulations listed above are best suited for different types of membrane configurations. Direct methods are practical only for extremely thin membranes, typically 10−100 nm,[5,9,17,23,31] where the net transmembrane fluxes are large. A complication that arises for ultrathin membranes is that the mass transfer resistance is not necessarily dominated by intracrystalline diffusion, for the surface barriers become crucial and may even dominate the mass transfer.[5,11,17,23] Direct calculations capture these effects explicitly, but their existence makes it challenging to extrapolate these results to membrane thicknesses typical of most experiments, where surface effects are typically thought to be minimal.[11,23]

The combined EMD-continuum approach to describing zeolite membranes, however, is valid only for membranes thick enough that surface barriers can be neglected.[12−14,16] The adsorption isotherm is used to define the boundary conditions, which assumes local surface equilibrium. In this case, the EMD approach has the strength that a complete description of the membrane performance as a function of feed and permeate pressure, feed composition, and so forth is available. Comparisons between this approach and experimental data for single-component and binary mixture permeance of light gases through thick silicalite membranes have yielded encouraging results.[13,16]

The comparison of the two atomically detailed modeling approaches above indicates that it would be very useful to have a direct means to determine the membrane thicknesses for which surface barriers are relevant. At present, the only means to achieve this goal is to perform direct simulations for progressively thicker membranes until results consistent with the absence of surface effects are observed.[5,11,17] Unfortunately, the membrane thicknesses that must be used with this approach

* Corresponding author. E-mail: sholl@andrew.cmu.edu.

10.1021/jp044247k CCC: $30.25
Published on Web 03/24/2005

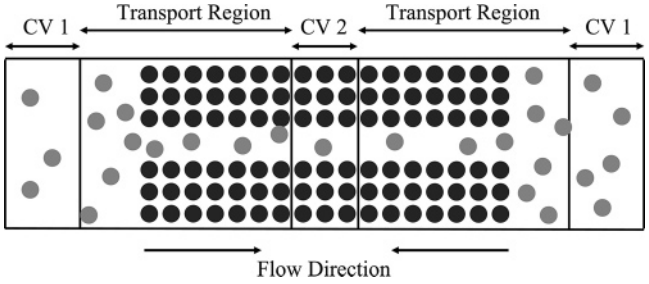

Figure 1. Schematic of the DCV-GCMD simulation box. Zeolite atoms are shown in black, and adsorbate atoms, in gray. Adsorbates are inserted into the higher-pressure control volume (CV 1), diffuse through the transport region, and are deleted in the low-pressure control volume (CV 2).

result in extremely time-consuming direct calculations,[5,32] even though they are typically much thinner than membranes that can be achieved in experimental practice.[3] In this paper, we present a different strategy to identify the regime where surface barriers can be neglected on the basis of performing EMD simulations of bulk zeolites and of zeolite/gas interfaces. When used in conjunction with EMD-based methods to describe gas permeance through zeolite membranes, the results presented below provide a practical means to predict the properties of zeolite membranes directly under the great majority of physical conditions relevant to practical uses of these membranes.

The paper is organized as follows. In section II, we describe dual control volume grand canonical molecular dynamics simulations we have performed to estimate membrane thicknesses for which surface barriers can be neglected during the permeation of CH_4 through silicalite. In section III, we describe an alternative approach to this issue that uses data from EMD simulations at the interface between a zeolite crystal and a bulk phase. The method is illustrated by reexamining the permeance of CH_4 and CF_4 through silicalite membranes. We discuss and compare the results for the two methods. The relative merits of these two approaches are discussed in section IV.

II. Dual Control Volume Grand Canonical Molecular Dynamics Simulations

A. Methodology. Dual control volume grand canonical molecular dynamics (DCV-GCMD) is a hybrid simulation technique that combines GCMC and MD to model nonequilibrium systems.[5−11,17−28] The simulation box, as seen in Figure 1, is divided into two control volumes, designated CV 1 and CV 2. GCMC is used to insert and delete molecules in the CVs to maintain the chemical potentials in each region. The CVs can be sustained at two different chemical potentials to create a concentration gradient across a membrane. We simulated a configuration in which both CV 2 and most of the transport region is filled with zeolite crystal. This configuration allows one to examine a membrane where the only surface resistance is associated with adsorption into the zeolite crystal.[5,17] We denote the gas-phase pressure corresponding to the chemical potential in CV 1 (CV 2) by P_1 (P_2).

In this study, we concentrated our DCV-GCMD runs on CH_4 diffusion in silicalite at $T = 298$ K. Adsorbate−adsorbate and adsorbate−zeolite interactions are modeled with the 12−6 Lennard-Jones pairwise potentials used previously by Skoulidas and Sholl.[14−16,33] The zeolite was assumed to be rigid. In the bulk zeolite region, we used a pretabulated look-up table and an interpolation scheme to compute the potential and forces rapidly. In the interfacial region, we make an explicit calculation of each adsorbate−zeolite interaction. The GCMC to MD ratio was kept at 20 moves/100 time steps for CV 1 and 1 move/500 time steps for CV 2 for all simulations. MD production times as long as 0.35 μs were used to establish that the flux measurements were converged.

To specify our simulations fully, we must describe how the surface of each zeolite membrane was defined. We follow earlier simulation studies[5,9,11,17,19,34,35] in simply truncating the crystal in a plane perpendicular to the transmembrane direction. The true surface structure of real zeolites may differ from this ideal, but accurately predicting these structures is beyond the scope of this work. Even for a single transmembrane direction, multiple surface terminations are possible when different truncation planes within the crystallographic unit cell are considered. For each membrane orientation, we performed a large series of EMD simulations to measure the equilibrium one-way flux across the membrane boundary when the zeolite is in equilibrium with gas-phase CH_4 at $P = 5$ bar and $T = 298$ K. All DCV-GCMD simulations were performed by choosing the truncation plane found to minimize the local density nearest the truncation plane. The one-way equilibrium flux is a parameter used in the alternative method to be described and is minimized when measured at the minimum local density plane. Because of periodic boundary conditions, the simulation volume exposes two distinct faces of the crystal because in the configuration that we used the low chemical potential CV lies in the middle of the zeolite crystal. The two surface truncations that gave the lowest pair of minimum densities were used for the two interfaces in the simulation volume. The flux measurements for the two interfaces were similar and were averaged to get the final results. In the results below, the transmembrane fluxes of each interface individually fell within the error bars of the averaged data points. For *x*-oriented membranes, two slightly different surfaces were exposed for reasons of computational convenience. At the gas−zeolite interface with gas on the left (right), the zeolite was truncated at 0.2*a* (0.4*a*), where *a* is the zeolite's unit cell length in the *x* direction. For comparison, we also performed simulations where both truncations were taken to be 0.5*a*, a location that bisects the *y*-oriented pores of the crystal. The interface resistances for this case were slightly less or equal to our base case, justifying the choice we made for the surface truncations at the minimum densities. For *y*-oriented membranes, the two truncation planes were 0.125*b* (left) and 0.94*b* (right). Both surfaces of the *z*-oriented membranes were truncated at 0.25*c*.

It is useful to note that the transmembrane flux in the absence of any surface resistances can be accurately calculated independently of our DVC-GCMD simulations. This flux, which we designate as the Fickian flux, J_{Fick}, is known once the adsorption isotherm and concentration-dependent Fickian diffusivity, $D_t(c)$, are known.[14] J_{Fick} is calculated by using these quantities as parametric input into Fick's law in integral form.[12] D_t and the adsorption isotherm for the model of CH_4 in silicalite we consider here have been computed previously by Skoulidas and Sholl.[13,14,16]

To reduce the computational costs of the DCV-GCMD simulations, we equilibrate the system using GCMC to populate the simulation box with molecules approximating the chemical potential profile that defines the Fickian flux. Specifically, we insert molecules to create a linear concentration profile across the membrane. This step is much more computationally efficient than starting the simulation with no molecules in the zeolite crystal and allowing molecules to diffuse into the zeolite membrane. Our GCMC equilibration uses $>5 \times 10^7$ MC moves to initialize the system. This was followed by a short period of

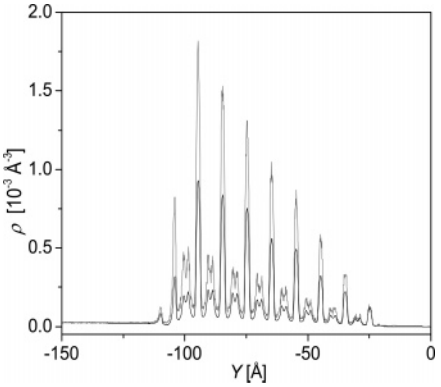

Figure 2. Density profile for CH_4 in a *y*-oriented silicalite crystal with $L = 8$ nm at $T = 298$ K. The gray profile is the initial GCMC profile. The black profile is the steady-state profile from DCV-GCMD.

MD equilibration and then an MD production period during which we measure the transmembrane flux. An example of this procedure is shown in Figure 2 for the case of CH_4 moving through a *y*-oriented membrane with thickness $L = 8$ nm at $T = 298$ K and $P_1 = 1$ bar and $P_2 = 0$ bar. The gray profile in Figure 2 is the initial condition from the GCMC equilibration. The black profile was measured during the MD production. The existence of a sizable surface barrier is evident in Figure 2 because the concentration gradient across the membrane at steady state is visibly smaller than that which would exist in the absence of any surface resistance. Similar results to those in Figure 2 are observed for other membrane orientations and thicknesses.

As discussed in earlier applications of DCV-GCMD,[9,10] the velocities of particles inserted in the control volumes must include a contribution from the appropriate thermal distribution and an additional streaming velocity, V_S. The streaming velocity should be chosen to match the net momentum flux across the CVs interfaces at steady state. The streaming velocity cannot be known a priori because it is related to the net transmembrane flux, which is the quantity the simulation aims to measure. We can, however, place an upper bound on the streaming velocity, $V_{S,Fick}$, by calculating the transmembrane flux in the absence of surface resistances, J_{Fick}, as described above. For each membrane thickness, we then performed an initial series of DCV-GCMD simulations with $V_S = \alpha V_{S,Fick}$ for $0 < \alpha < 1$. The correct streaming velocity is the one for which

$$\left(\frac{V_{S,Fick}}{V_S}\right)\left(\frac{J_{DCV}}{J_{Fick}}\right) = 1 \qquad (1)$$

where J_{DCV} is the flux measured with DCV-GCMD. Figure 3 shows an example of this type of calculation for a *y*-oriented membrane with $L = 8$ nm. The general characteristics seen in Figure 3 were also observed for the other membrane thicknesses and orientations we examined. In the specific example in Figure 3, the correct streaming velocity is ~40% of $V_{S,Fick}$. All fluxes reported below were calculated after determining the appropriate streaming velocity in this way.

A final technical detail in DCV-GCMD is the choice of thermostat. In our simulations, as in many other simulations of molecular diffusion in zeolites, the zeolite framework is held rigid to reduce computational expense. This can create unphysical effects at zeolite crystal interfaces. For example, as molecules move from the gas phase toward the zeolite, they are greatly accelerated by the drop in potential energy of their environment. In a real system, this gain in kinetic energy rapidly dissipates during collisions with the crystal. In a rigid zeolite simulation,

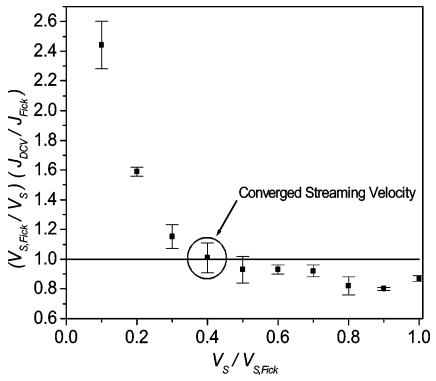

Figure 3. Data used to establish the applied streaming velocity V_S for the case of CH_4 in the *y* orientation at $T = 298$ K and $L = 8$ nm.

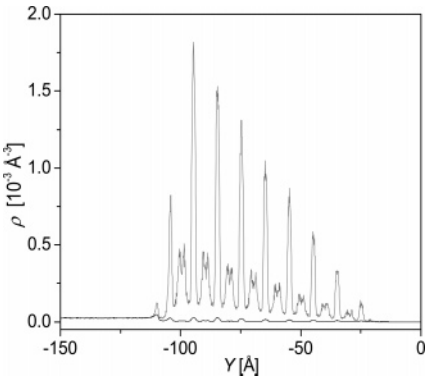

Figure 4. Same as Figure 2, but for a DCV-GCMD simulation in which the localized Andersen thermostat is absent.

however, this crucial channel for energy exchange is absent. Any thermostat that acts only on the global average kinetic energy, such as the Nosé−Hoover thermostat[9,36−38] or velocity rescaling,[5,17,38] cannot correct for this difficulty. With these methods, the global average temperature is controlled, but significant spatial inhomogeneities in the local temperature profile persist at steady state. Test calculations we performed with the two global thermostats mentioned above indicated that these effects can strongly influence the observed steady-state flux. An extreme example is shown in Figure 4 for a *y*-oriented membrane with $L = 8$ nm. In this example, no thermostat was used apart from the temperature control inherent in the GCMC insertions. The density profile resulting from this simplistic approach is very strongly depleted relative to the result in the absence of an adsorption resistance. If taken at face value, these data would be interpreted as evidence of a very large adsorption resistance. In reality, the local temperature profile in this simulation was strongly isothermal, so the data cannot be meaningfully interpreted in terms of permeation through a membrane under isothermal conditions.

To address this thermostat issue while maintaining the computational convenience of the rigid zeolite, we imposed a localized thermostat in the interfacial region that mimics collisional energy transfer between molecules and the zeolite. Specifically, we apply an Andersen thermostat[38] to all molecules inside the bulk gas outside of the CV 1 and within a distance $R_c = 13$ Å of the membrane's plane of truncation inside the zeolite membrane. Whenever new velocities are assigned with this local thermostat, the streaming velocity is added to the molecule's total velocity. The collision frequency of the Andersen thermostat was chosen to be roughly the inverse of the surface layer residence time. When using this scheme, no other thermostat was applied to molecules in the transport

region. This method yields accurate global temperature control with a high degree of spatial homogeneity in the temperature profile. The results shown in Figure 2 and all DCV-GCMD results shown below were generated using this method.

B. Flux Measurement Results. Once the correct streaming velocity was established and the local Andersen thermostat was applied, we used DCV-GCMD to measure the fluxes of CH_4 in the *x*, *y*, and *z* orientations of silicalite membranes for four thicknesses, $L = 8$, 16, 32, and 64 nm. In every case, the feed pressure was 1 bar, and the pressure drop across the membrane was also 1 bar. As mentioned above, our simulations were configured so the only surface resistance to membrane transport is associated with adsorption into the membrane. Three planes were set up in each membrane, and the local flux of molecules moving from left to right and right to left was measured by counting the number of molecules crossing over each of the planes. The difference between the two fluxes is the transmembrane flux. Each reported flux below is an average of the six measured fluxes.

To establish that our DCV-GCMD simulations reached a converged steady-state value, we measured the flux for a set of increasing production times. In Figure 5, we show the measured flux for CH_4 in the *y* orientation for the four thicknesses as a function of the dimensionless production time, t^*, defined as

$$t^* = \frac{t_{\mathrm{Prod}}}{t_{\mathrm{Diff}}} \tag{2}$$

Here, t_{Prod} is the MD production time, and $t_{\mathrm{Diff}} = L^2/(D_t)$ is the characteristic diffusion time for the membrane, where D_t is the infinite dilution CH_4 diffusivity in the transmembrane direction. The runs for $L = 64$ nm with $t^* = 2.5$ correspond to an MD production time of 350 ns. The results in Figure 5 indicate that the steady state has been reached in each case for the longest simulation times, and data from these simulations was used to assess the adsorption resistance of each membrane.

To define the adsorption resistance, we first calculate the net flux in the absence of surface barriers, J_{Fick}, using the Fickian diffusion coefficients available from previous EMD studies of CH_4 diffusion in silicalite.[14] This approach includes the orientational and concentration dependence of the transport diffusivities. J_{Fick} is used to define the intracrystalline resistance, R_{intra}, by

$$J_{\mathrm{Fick}} = \frac{1}{R_{\mathrm{intra}}}\frac{\Delta P}{RT} \tag{3}$$

Similarly, the observed flux from DCV-GCMD defines the total membrane resistance through

$$J_{\mathrm{DCV}} = \frac{1}{R_{\mathrm{tot}}}\frac{\Delta P}{RT} \tag{4}$$

By writing the total membrane resistance as the sum of an adsorption resistance and the intracrystalline resistance, $R_{\mathrm{tot}} = R_{\mathrm{intra}} + R_{\mathrm{ads}}$, the two equations above can be used to determine R_{ads} unambiguously.

Our main interest is the magnitude of the adsorption resistance relative to the intracrystalline resistance. Accordingly, in Figures 6−8 we plot $R_{\mathrm{ads}}/R_{\mathrm{intra}}$ for *y*-, *x*-, and *z*-oriented membranes, respectively. In each case, the filled symbols are our DCV-GCMD results. As expected, the surface resistances are large for extremely thin membranes. For $L = 8$ nm, $R_{\mathrm{ads}} > R_{\mathrm{intra}}$ for the *y*- and *x*-oriented membranes.

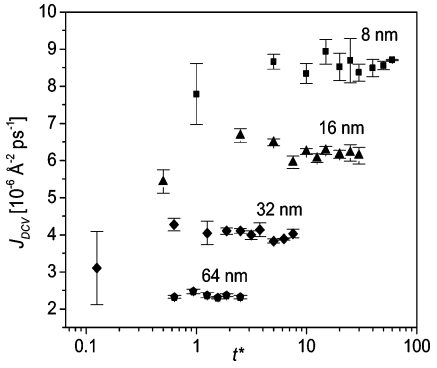

Figure 5. Transmembrane flux for CH_4 through *y*-oriented membranes as a function of membrane thickness and production time. The production time is normalized by the characteristic diffusion time, t_{Diff}, as described in the text.

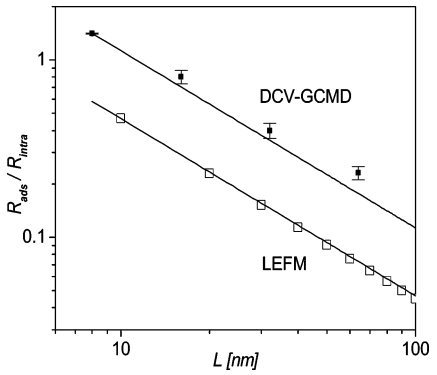

Figure 6. $R_{\mathrm{ads}}/R_{\mathrm{intra}}$ for CH_4 at $T = 298$ K in the *y* orientation as a function of membrane thickness *L* (nm) computed using DCV-GCMD (filled symbols) and the LEFM (open symbols). The solid lines show a $^1/_L$ scaling extrapolated from the results with the $L = 8$ nm point.

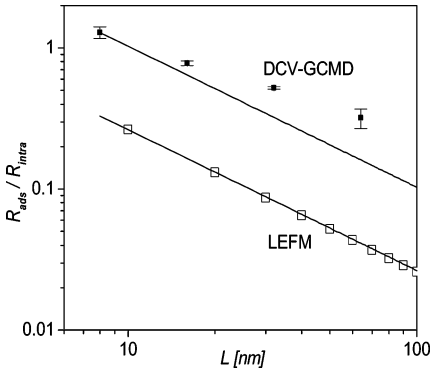

Figure 7. Same as Figure 6, but for CH_4 in the *x* orientation.

For fixed feed and permeate conditions, $R_{\mathrm{intra}} \propto L$.[5,17] Hence, if R_{ads} is independent of *L*, $(R_{\mathrm{ads}}/R_{\mathrm{intra}}) \propto L^{-1}$. This scaling is shown in Figures 6−8 by the solid line passing through the DCV-GCMD result for $L = 8$ nm. For the *y*- and *x*-oriented membranes, the DCV-GCMD data show that R_{ads} is approximately independent of *L* for the conditions studied. This is a useful conclusion because it can immediately be used to determine the membrane thicknesses beyond which the adsorption resistance is negligible. For *y*-oriented membranes, $R_{\mathrm{ads}}/R_{\mathrm{intra}}$ is predicted to be 0.1 for $L = 137$ nm and 0.01 for $L = 1370$ nm.

Our DCV-GCMD simulations for *z*-oriented membranes are more problematic than for the other two membrane orientations. As is well established, CH_4 diffuses through silicalite approximately an order of magnitude slower in the *z* orientation than in the *x* or *y* orientations because of the tortuous path

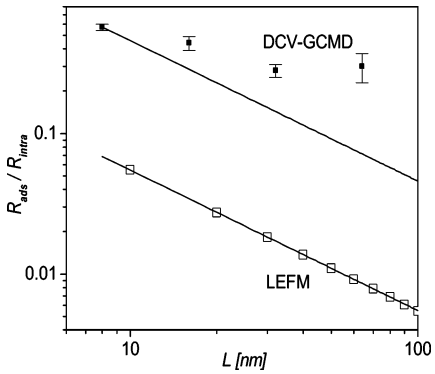

Figure 8. Same as Figure 6, but for CH_4 in the *z* orientation.

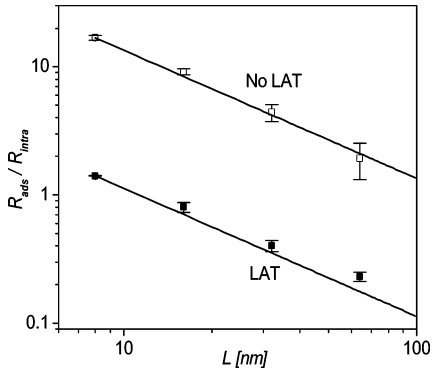

Figure 9. R_{ads}/R_{intra} for CH_4 at $T = 298$ K in the *y* orientation as a function of membrane thickness *L* (nm) computed using DCV-GCMD with and without the localized Andersen thermostat (LAT), as shown by filled and open symbols, respectively.

molecules must follow to make net motion in the *z* direction.[14] As a result, the absolute fluxes observed in our DCV-GCMD simulations of *z*-oriented membranes are small. For example, the total flux of molecules observed for our *z*-oriented membrane with $L = 64$ nm during 350 ns of simulation time was only ~160 molecules. To make matters worse, the slow intracrystalline diffusion limits the dimensionless times, t^*, that are accessible in our calculations. For $L = 64$ nm, the simulation just described corresponds to only $t^* = 0.3$. Because of these factors, the DCV-GCMD results for $L > 8$ nm in Figure 8 should be viewed with skepticism, although we report them here for completeness. Although the data in Figure 8 indicate that R_{ads} is not independent of *L*, we feel that this may be a shortcoming of the simulations rather than a physically accurate result.

To reiterate the necessity of applying a local thermostat in the interface region of the DCV-GCMD simulations, we show in Figure 9 results for *y*-oriented membranes with and without the localized Andersen thermostat (LAT) defined above. The data from simulations with the thermostat are the same as those in Figure 6. Not applying the thermostat causes the adsorption resistance to be overestimated by roughly an order of magnitude. An examination of the simulations without the thermostat shows the presence of strong deviations from isothermal conditions in the interface region, even though the global average temperature of each simulation was acceptable. The implication of these observations is that results from previous DCV-GCMD studies of zeolite membranes that did not apply any kind of local thermostat in the interface region should be treated with caution. It would be interesting in the future to directly compare results based on the localized thermostat defined above with simulations where the zeolite framework is treated as fully flexible.

III. Local Equilibrium Flux Method

The results above point to several disadvantages of DCV-GCMD simulations for assessing surface resistances in nanoporous membranes. These simulations are very time-consuming, even though they probe membranes that are only a fraction of the film thickness relevant in practical experiments.[5,9,11,17,31,32] Care must be taken in these simulations to correctly describe technical issues such as streaming velocities and collisional energy transfer. The latter issue is relevant only in simulations where the membrane material is held rigid for computational efficiency. A more subtle disadvantage is that DCV-GCMD gives results only for specific membrane operating conditions. All of the results above deal with feed pressures and pressure drops of 1 bar. To determine what surface resistances exist at, say, a feed pressure of 8 bar and a pressure drop of 4 bar, completely independent and time-consuming simulations would be required.

We introduce below a method to estimate surface resistances in nanoporous membranes that aims to address some of the drawbacks of DCV-GCMD. The twin aims of this method are to use a fully atomically detailed description of adsorbates and membrane materials and to provide a way to assess arbitrary operating conditions and membrane thicknesses rapidly. We explicitly aim to provide only an estimate of the surface resistances, with the idea that the accuracy of the method can be established by comparison to DCV-GCMD simulations in a regime where these simulations are feasible.

Two approximate treatments of surface resistances are already available. Barrer used a phenomenological model of molecules hopping between external and internal sites to derive expressions for surface resistances.[39] This model gives excellent insight into the types of behaviors that can exist, but no means to directly connect this model with atomically detailed models are available. Maginn et al. computed the free-energy profiles of molecules leaving the pores of $AlPO_4$-5 and showed how these profiles could be connected with the desorption resistances associated with these molecules.[11] This approach includes atomic-scale detail, but it is difficult to extend in a natural way to arbitrary adsorbate densities, limiting the operating conditions to which it can be applied.

Our approach, which we will refer to as the local equilibrium flux method (LEFM), is formulated in terms of the one-way fluxes across planes perpendicular to the transmembrane direction. We define the one-way flux across an arbitrary plane from left to right (right to left) as j_+ (j_-). The difference between these two fluxes is, of course, the net flux, $J = j_+ - j_-$. Under equilibrium conditions, $j_+ = j_- = j^{eq}$, and this one-way flux can be readily observed from an atomically detailed model using equilibrium MD. An example of this measured flux for the pore mouth of a *y*-oriented silicalite membrane as a function of CH_4 pressure at $T = 298$ K is shown in Figure 10. The one-way fluxes j^{eq} were measured in simulations that used the same localized Andersen thermostat as in our DCV-GCMD simulations.

To estimate the surface resistance, we posit that the net flux under steady-state nonequilibrium conditions can be described by the difference in one-way equilibrium fluxes at different effective pressures. That is,

$$J = j_- - j_+ \cong j^{eq}(P_{feed}) - j^{eq}(P_{surf}) \qquad (5)$$

Here, P_{feed} is the actual gas-phase pressure outside the membrane, and P_{surf} is the (as yet unspecified) effective pressure in the membrane boundary layer. Viewing P_{surf} as a perturbation

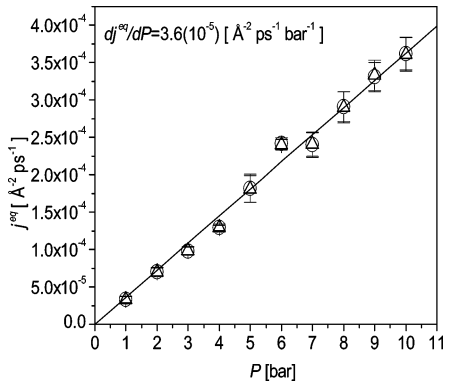

Figure 10. Local one-way surface flux for CH_4 in the *y* orientation at $T = 298$ K measured using EMD. Circles and triangles represent one-way fluxes entering and leaving the crystal, respectively. The two surface terminations used gave similar one-way fluxes. The absolute smallest set of values were used in the LEFM.

about P_{feed} by writing $P_{surf} = P_{feed} - \delta P$, we can write to first order in δP

$$j^{eq}(P_{surf}) = j^{eq}(P_{feed} - \delta P) \cong j^{eq}(P_{feed}) - \delta P\left(\frac{dj^{eq}}{dP}\bigg|_{P_{feed}}\right) \quad (6)$$

Combining the two equations above gives

$$J \cong \delta P\left(\frac{dj^{eq}}{dP}\bigg|_{P_{feed}}\right) \quad (7)$$

At steady state, the same net flux must exist inside the membrane, where it can be defined via the integral form of Fick's law,

$$J = \frac{1}{L}\int_{c(P_{perm})}^{c_{surf}} D_t(c')\, dc' \quad (8)$$

Here, $c(P_{perm})$ is the adsorption isotherm evaluated at the permeate pressure P_{perm}, and c_{surf} is the feed-side zeolite concentration that is at equilibrium with the gas at effective pressure P_{surf}. To estimate the net transmembrane flux in the presence of an adsorption resistance, we find a self-consistent solution to eqs 7 and 8. Once this flux is known, the adsorption resistance can be determined as it was in analyzing the DCV-GCMD simulations described above.

It is useful to note that with some mild assumptions the adsorption resistance predicted by the LEFM can be written in an analytic form. The integral form of Fick's law can be rewritten as

$$JL = \int_{c_{perm}}^{c_{feed}} D_t(c')\, dc' - \int_{c_{ext}}^{c_{feed}} D_t(c')\, dc' = J_{Fick}L - \int_{c_{ext}}^{c_{feed}} D_t(c')\, dc' \quad (9)$$

where c_{ext} is the adsorbate concentration in the zeolite in equilibrium with a gas-phase region at pressure P_{ext}. If we assume that the concentration change from c_{feed} to c_{ext} is small, then

$$\int_{c_{ext}}^{c_{feed}} D_t(c')\, dc' \cong \delta c D_t(c_{feed}) \quad (10)$$

This expression is valid provided that the diffusivity does not change rapidly with concentration in the range of the integral. One way to approximate dj^{eq}/dP is to assume it can be represented by a constant, α. We will show below that for the examples we have examined this is a reasonable assumption over a broad range of pressures. The solution of the LEFM must satisfy

$$\alpha \delta c\left(\frac{dP}{dc}\right)|_{P_{feed}} L \cong J_{Fick}L - \delta c D_t(c_{feed}) \quad (11)$$

This expression allows the adsorption resistance to be expressed in a simple form,

$$\frac{R_{ads}}{R_{intra}} = \frac{J_{Fick}}{J} - 1 \cong \frac{D_t(c_{feed})}{\alpha L\left(\frac{dP}{dc}\right)_{P_{feed}}} \quad (12)$$

This expression can be further simplified by using the corrected diffusivity, $D_0(c)$, which is related to the Fickian diffusivity without approximation by

$$D_t(c) = D_0(c)\frac{d \ln P}{d \ln c} \quad (13)$$

In terms of the corrected diffusivity,

$$\frac{R_{ads}}{R_{intra}} \cong \frac{D_0(c_{feed})}{\alpha L}\frac{c}{P} \quad (14)$$

We reiterate that this expression has been derived by assuming that the concentration change in the zeolite boundary layer due to the adsorption resistance is small and that $dj^{eq}/dP \cong \alpha$. When these conditions are satisfied, we find that $(R_{ads}/R_{intra}) \propto L^{-1}$ for constant feed conditions. We can also see in general that (R_{ads}/R_{intra}) will decrease if the feed pressure is increased because the adsorbate concentration does not increase linearly with pressure for pressures outside the Henry's law regime of the adsorption isotherm and the corrected diffusivity has been found in numerous examples to be either constant or decreasing as the adsorbate concentration is increased.[14,15,24,33]

We have presented eq 14 because it gives useful insight into the scaling of adsorption resistances, but it is not necessary to use this approximate result to predict the actual adsorption resistances in the examples we study below. In all of our detailed calculations, we accurately evaluated the integral in eq 8 using the concentration dependence of the diffusivity and used a functional form for dj^{eq}/dP determined from detailed simulations of the system of interest.

Once j^{eq} has been determined as a function of P, the LEFM process just defined is straightforward to apply for any set of operating conditions and membrane thickness without needing any additional atomistic simulations. The description above applies to membranes with only an adsorption resistance because this is the case we treated in detail with our DCV-GCMD simulation. There is no conceptual barrier to extending the LEFM to combined adsorption/desorption resistances or to multicomponent permeance.

The open symbols in Figures 6−8 show the predictions of the LEFM with our DCV-GCMD results for CH_4 permeances through silicalite membranes at $T = 298$ K oriented in the *y*, *x*, and *z* orientations, respectively. In each case, the solid curve was obtained by taking the LEFM results from $L = 10$ nm and assuming that $(R_{ads}/R_{intra}) \propto L^{-1}$ for other membrane thicknesses. The full LEFM calculations are seen to obey this scaling quite accurately. That is, the LEFM calculations predict that the adsorption resistance for each membrane is essentially independent of membrane thickness.

The accuracy of the LEFM estimates can be examined by comparing them to our DCV-GCMD results, which can be

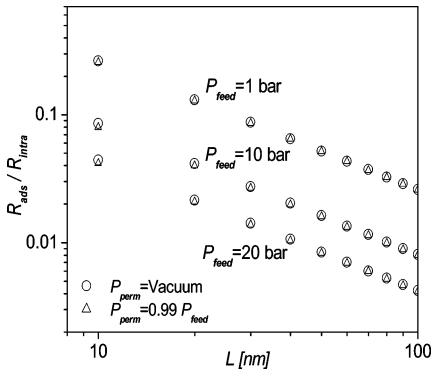

Figure 11. R_{ads}/R_{intra} for CH_4 in the *x* orientation at $T = 298$ K as calculated with the LEFM for $P_{feed} = 1$, 10, and 20 bar and for $P_{perm} = 0$ bar (circles) and 99% of the P_{feed} (triangles).

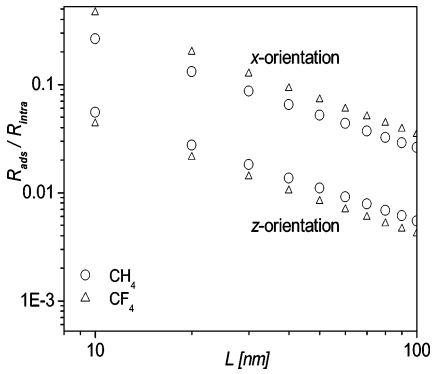

Figure 12. R_{ads}/R_{intra} for CH_4 and CF_4 in the *x* and *z* orientations at $T = 298$ K as calculated with the LEFM for $P_{feed} = 1$ bar and $P_{perm} = 0$ bar.

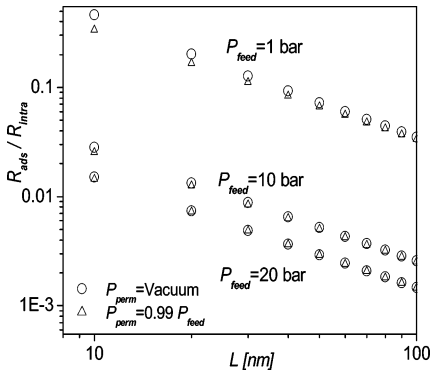

Figure 13. Same as Figure 11, but for CF_4 in the *x* orientation.

treated as direct measurements of the actual adsorption resistance. In every case, the LEFM underestimates the magnitude of the adsorption resistance. For both *y*- and *x*-oriented membranes, the LEFM underestimates the adsorption resistance by approximately a factor of 3. For the *z*-oriented membrane, the discrepancy is larger, with the LEFM underestimating the adsorption resistance by roughly a factor of 7 for the membrane thickness where we have the most confidence in our DCV-GCMD results ($L = 8$ nm). We have examined several generalizations of the LEFM, for example, continuing eq 6 to second order in δP, but these have not yielded greatly improved results.

Despite the quantitative discrepancies between the actual adsorption resistances and the LEFM predictions, we feel that the LEFM will provide a useful tool for understanding when surface resistances may be important in practical experiments. It is important to note that the simulation effort required to generate all of the LEFM data in Figure 6 is less than the effort required to accumulate data for a single DVC-GCMD data point. Furthermore, once data in Figure 10 has been gathered for the membrane surface of interest, applying the LEFM to arbitrary membrane operating conditions and thicknesses is very simple. As an example of this property, Figure 11 shows the LEFM predictions for CH_4 permeation through an *x*-oriented silicalite membranes with three different feed pressures, 1, 10, and 20 bar. In this Figure, the circles are the results for membranes with a pressure drop equal to the feed pressure, and the triangles are for membranes where the pressure drop is only 1% of the feed pressure. The latter condition would be essentially impossible to probe with DCV-GCMD simulations because of the small driving force for permeation and resulting small absolute fluxes. A useful observation from Figure 11 is that the adsorption resistance is essentially independent of the downstream conditions, as suggested by eq 14. The resistances shown in Figure 11 therefore describe all possible operating conditions with feed pressures lower than 20 bar. The importance of the adsorption resistance relative to the intracrystalline resistance is reduced as the feed pressure is increased. This observation can also be understood from eq 14 because as P increases and the adsorption isotherm saturates, c/P decreases and the corrected diffusivity for CH_4, a quantity measured in previous EMD simulations,[14,24,33] is a weakly decreasing function of P.

As a second demonstration of the ease of use of the LEFM, we have applied it to the permeance of CF_4 through silicalite membranes. The adsorption and diffusion of CF_4 in silicalite, both as a single component and in mixtures with CH_4, has been extensively studied in previous atomistic simulations.[14,40] We used the same interatomic potentials as in this previous work and used the transport diffusivities previously computed using EMD by Skoulidas and Sholl.[14,40] The adsorption resistances predicted for CF_4 through *x*- and *z*-oriented membranes are compared with the analogous results for CH_4 in Figure 12 for membranes with $P_{feed} = 1$ bar and a pressure drop of 1 bar. The relative importance of adsorption resistances under these conditions is predicted to be comparable for CF_4 and CH_4.

The variation in the LEFM-predicted adsorption resistances for CF_4 as a function of feed pressure and pressure drop for an *x*-oriented membrane is shown in Figure 13. As with CH_4, the variation in the adsorption resistance with pressure drop is predicted to be very small. The adsorption resistance varies more strongly as a function of feed pressure than was found for CH_4, as can be seen by comparing Figures 11 and 13. As P is increased from 1 to 10 bar, the variation in R_{ads}/R_{intra} is more dramatic for CF_4 than for CH_4. This can be understood from eq 14 by noting that the CF_4 isotherm at the temperature of interest saturates more rapidly and the corrected diffusivity of CF_4, as measured in previous EMD simulations,[14,15,33] drops strongly with increasing concentrations. As a result, $(D_0(c)c)/P$ decreases much more rapidly as P is increased from 1 to 10 bar for CF_4 than for CH_4.

IV. Conclusions

We have compared two methods for estimating the resistance to mass transfer as molecules diffuse through the gas−zeolite interfaces of zeolite membranes from atomically detailed principles. In both cases, we focused on the adsorption of simple spherical species into silicalite membranes at room temperature, although there is no conceptual barrier to applying either method to more complex adsorbates or adsorbents.

DCV-GCMD is a well-established technique that can in principle directly measure transmembrane fluxes with atomic

detail. We have illustrated several pitfalls in applying this technique, most notably the strong dependence on the observed flux as the means used to mimic collisional energy transfer between adsorbates and the solid in the interface region. DCV-GCMD simulations that use only global thermostats can exhibit strong nonisothermal effects even under conditions of steady-state flow, and we have given an example of how this can dramatically affect the surface resistance that is inferred from simulations. We applied a simple local thermostat that mimics collisional energy transfer in the interface region while holding all atoms in the adsorbent rigid. It would be useful to compare results from this method with more detailed calculations that include these effects in a less approximate manner, but maintaining the computational efficiency of DCV-GCMD is extremely important in view of the very long simulations that need to be performed to describe membranes that from an experimental point of view are extraordinarily thin.

We have introduced an approximate method that aims to bypass the computational expense of DCV-GCMD while still retaining an atomically detailed description of the membrane material. This so-called Local Equilibrium Flux Method (LEFM) uses information on the one-way fluxes across the zeolite−gas interface under equilibrium conditions and the concentration-dependent transport diffusion coefficients for the adsorbate in the bulk of the membrane material. All of this information is readily available from atomically detailed EMD simulations. Although it is approximate, the LEFM is a useful complement to DCV-GCMD simulations because it can be applied extremely rapidly to estimate the surface resistances associated with a membrane for essentially any feed pressure and permeate pressure.

The LEFM is not an exact method. In a series of comparisons between the LEFM and DCV-GCMD for a series of examples where both methods are applicable, the LEFM underestimated the adsorption resistance for CH_4 into silicalite by a factor of 3−7. We claim that this level of accuracy is enough to allow the LEFM to be useful for answering practical questions related to the design and interpretation of zeolite membrane experiments. The most relevant issue in this arena is simply whether surface resistances have a significant impact on the outcome of a particular series of experiments. As an example, we can consider this question for the transport of CH_4 or CF_4 through silicalite crystals that can appear in practical membranes. The lower size limit[3] for crystals of this type is ~ 1 μm, and most membranes to date are composed of crystals that are considerably larger than this limit. Our LEFM calculations indicate that for these crystals the adsorption resistances under all practical operating conditions (feed and permeate pressure) are at least 2 orders of magnitude smaller than the intracrystalline resistance and can therefore be neglected. Under these circumstances, being able to predict the surface resistance within a factor of 3−7 is certainly sufficient to establish the relevance of these effects to real experiments.

It is reasonable to expect that there are practical situations where surface resistances will be important. Recent work on the synthesis of nanosized zeolite particles,[41] for example, has created materials where net mass transfer into and out of the particles is likely to be strongly effected by surface barriers. In these instances, the LEFM will be useful as a numerical tool to assess the relative importance of intracrystalline and surface resistances rapidly. When the latter are determined to be significant, DCV-GCMD could then be used to assess the precise magnitude of these resistances accurately.

Acknowledgment. This work was supported by the NSF (CTS-0413027). Crucial feedback on an early version of this work from Dr. Aidan Thompson is gratefully acknowledged.

References and Notes

(1) Auerbach, S. M. *Int. Rev. Phys. Chem.* **2000**, *19*, 155.
(2) Matsukata, M.; Kikuchi, E. *Bull. Chem. Soc. Jpn.* **1997**, *70*, 2341.
(3) Tsapatsis, M.; Vlachos, D. G.; Thompson, R.; Terasaki, O.; Kokkoli, E.; M., A.; Sujaoti, K.; Nery, J.; Diaz, I.; Bonilla, G.; Lai, Z. *Science* **2003**, *300*, 456.
(4) Coronas, J.; Santamaria, J. *Sep. Purif. Methods* **1999**, *28*, 127.
(5) Ahunbay, M. G.; Elliott, J. R.; Talu, O. *J. Phys. Chem. B* **2002**, *106*, 5163.
(6) Pohl, P. I.; Heffelfinger, G. S. *J. Membr. Sci.* **1999**, *155*, 1.
(7) Pohl, P. I.; Heffelfinger, G. S.; Smith, D. M. *Mol. Phys.* **1996**, *89*, 1725.
(8) Takaba, H.; Koshita, R.; Mizukami, K.; Oumi, Y.; Ito, N.; Kubo, M.; Fahmi, A.; Miyamoto, A. *J. Membr. Sci.* **1997**, *134*, 127.
(9) Martin, M. G.; Thompson, A. P.; Nenoff, T. M. *J. Chem. Phys.* **2001**, *114*, 7174.
(10) Arya, G.; Chang, H. C.; Maginn, E. J. *J. Chem. Phys.* **2001**, *115*, 8112.
(11) Arya, G.; Maginn, E. J.; Chang, H. C. *J. Phys. Chem. B* **2001**, *105*, 2725.
(12) Sholl, D. S. *Ind. Eng. Chem. Res.* **2000**, *39*, 3737.
(13) Bowen, T. C.; Falconer, J. L.; Noble, R. D.; Skoulidas, A. I.; Sholl, D. S. *Ind. Eng. Chem. Res.* **2002**, *41*, 1641.
(14) Skoulidas, A. I.; Sholl, D. S. *J. Phys. Chem. B* **2002**, *106*, 5058.
(15) Skoulidas, A. I.; Sholl, D. S. *J. Phys. Chem. B* **2003**, *107*, 10132.
(16) Skoulidas, A. I.; Sholl, D. S.; Bowen, T. C.; Doelling, C.; Falconer, J. L.; Noble, R. D. *J. Membr. Sci.* **2003**, *227*, 123.
(17) Ahunbay, M. G.; Elliott, J. R.; Talu, O. *J. Phys. Chem. B* **2004**, *108*, 7801.
(18) Furukawa, S.; McCabe, C.; Nitta, T.; Cummings, P. T. *Fluid Phase Equilib.* **2002**, *194*−*197*, 309.
(19) Mizukami, K.; Kobayashi, Y.; Morito, H.; Takami, S.; Kubo, M.; Belosludov, R.; Miyamoto, A. *Jpn. J. Appl. Phys., Part 1* **2000**, *39*, 4385.
(20) Furukawa, S.; Nitta, T. *J. Chem. Eng. Jpn.* **2003**, *36*, 313.
(21) Cracknell, R. F.; Nicholson, D.; Quirke, N. *Phys. Rev. Lett.* **1995**, *74*, 2463.
(22) MacElroy, J. M. D.; Boyle, M. J. *Chem. Eng. J.* **1999**, *74*, 85.
(23) Murad, S.; Lin, J. *Ind. Eng. Chem. Res.* **2002**, *41*, 1076.
(24) Maginn, E. J.; Bell, A. T.; Theodorou, D. N. *J. Phys. Chem. B* **1993**, *97*, 4173.
(25) Zhang, Q.; Zheng, J.; Shevade, A.; Zhang, L.; Gehrke, S.; Heffelfinger, G. S.; Jiang, S. *J. Chem. Phys.* **2002**, *117*, 808.
(26) Xu, L. F.; Tsotsis, T. T.; Sahimi, M. *J. Chem. Phys.* **1999**, *111*, 3252.
(27) Xu, L. F.; Sedigh, M. G.; Tsotsis, T. T.; Sahimi, M. *J. Chem. Phys.* **2000**, *112*, 910.
(28) Xu, L. F.; Sedigh, M. G.; Sahimi, M.; Tsotsis, T. T. *Phys. Rev. Lett.* **1998**, *80*, 3511.
(29) Suzuki, S.; Nagumo, R.; Takaba, H.; Nakao, S. *Microporous Mesoporous Mater.* **2001**, *48*, 247.
(30) Suzuki, S.; Takaba, H.; Yamaguchi, T.; Nakao, S. *J. Phys. Chem. B* **2000**, *104*, 1971.
(31) Snyder, M. A.; Vlachos, D. G.; Katsoulakis, M. A. *Chem. Eng. Sci.* **2003**, *58*, 895.
(32) Tunca, C.; Ford, D. M. *J. Chem. Phys.* **2004**, *120*, 10763.
(33) Skoulidas, A. I.; Sholl, D. S. *J. Phys. Chem. B* **2001**, *105*, 3151.
(34) Chandross, M.; Webb, E. B.; Grest, G. S.; Martin, M. G.; Thompson, A. P.; Roth, M. W. *J. Phys. Chem. B* **2001**, *105*, 5700
(35) Webb, E. B.; Grest, G. S. *J. Chem. Phys.* **2002**, *116*, 6311.
(36) Nose, S. *J. Chem. Phys.* **1984**, *81*, 511.
(37) Hoover, W. G. *Phys. Rev. A* **1985**, *31*, 1695.
(38) Frenkel, D.; Smit, B. *Understanding Molecular Simulation: From Algorithms to Applications*, 2nd ed.; Academic Press: San Diego, CA, 2002.
(39) Barrer, R. Zeolites as Membranes: The Role of the Gas-Crystal Interface. In *Catalysis and Adsorption by Zeolites*; Öhlmann, G., Pfeifer, H., Fricke, R., Eds.; Elsevier Science Publishers: New York, 1991; p 257.
(40) Skoulidas, A. I.; Sholl, D. S.; Krishna, R. *Langmuir* **2003**, *19*, 7977.
(41) Song, W.; Justice, R. E.; Jones, C. A.; Grassian, V. H.; Larsen, S. C. *Langmuir* **2004**, *20*, 8301.